THE JOURNAL OF BIOLOGICAL CHEMISTRY
Vol. 280, No. 34, Issue of August 26, pp. 30581–30585, 2005

Printed in U.S.A.

Structural and Chemical Requirements for Histidine Phosphorylation by the Chemotaxis Kinase CheA*

Received for publication, May 16, 2005, and in revised form, June 24, 2005
Published, JBC Papers in Press, June 30, 2005, DOI 10.1074/jbc.M505316200

Cindy M. Quezada‡, Damon J. Hamel§, Cristian Grădinaru¶, Alexandrine M. Bilwes¶, Frederick W. Dahlquist§, Brian R. Crane¶, and Melvin I. Simon‡‖

From the ‡Division of Biology, California Institute of Technology, Pasadena, California 91125, the ¶Department of Chemistry and Chemical Biology, Cornell University, Ithaca, New York 14853, and the §Department of Chemistry and Biochemistry, University of California, Santa Barbara, California 93106

The CheA histidine kinase initiates the signal transduction pathway of bacterial chemotaxis by autophosphorylating a conserved histidine on its phosphotransferase domain (P1). Site-directed mutations of neighboring conserved P1 residues (Glu-67, Lys-48, and His-64) show that a hydrogen-bonding network controls the reactivity of the phospho-accepting His (His-45) in *Thermotoga maritima* CheA. In particular, the conservative mutation E67Q dramatically reduces phosphotransfer to P1 without significantly affecting the affinity of P1 for the CheA ATP-binding domain. High resolution crystallographic studies revealed that although all mutants disrupt the hydrogen-bonding network to varying degrees, none affect the conformation of His-45. ^{15}N-NMR chemical shift studies instead showed that Glu-67 functions to stabilize the unfavored $N^{\delta 1}H$ tautomer of His-45, thereby rendering the $N^{\epsilon 2}$ imidazole unprotonated and well positioned for accepting the ATP phosphoryl group.

Histidine phosphorylation is a key feature of bacterial signaling. Histidine kinases transduce information from the extracellular environment to regulate many cellular processes including gene expression, membrane permeability, energy production, and motility (1–3). Mammals do not contain histidine kinases homologous to those found in prokaryotes. Thus, these enzymes are attractive targets for the development of new antibiotics, and thus, their catalytic mechanisms hold great interest.

The dimeric histidine kinase CheA initiates the phosphorylation cascade that regulates the directed movement of bacteria toward and away from chemical stimulants. All necessary elements for histidine phosphorylation are found in the phosphotransfer (P1) and kinase (P4) domains of the five-domain CheA protein (4). Conserved residues in the P4 domain bind ATP in a pocket that optimally positions the γ-phosphoryl for transfer to a specific histidine on the N-terminal P1 domain (4, 5). Although P1 residues other than the active histidine have been shown to impact phospho-transferase activity, their chemical functions have not been assigned (6).

The structure of CheA domain P4 revealed no similarity to eukaryotic Ser/Thr or Tyr kinases but significant resemblance to ATPases from the functionally divergent GHL[1] family (for GyrB, Hsp90, MutL) (4, 7). Instead of using ATP as a phosphodonor to histidine, the GHL ATPases effectively transfer the ATP γ-phosphoryl group to a water molecule. CheA and the GHL family of ATPases share similar topologies, a deep cavity for ATP binding, and four regions of sequence conservation surrounding the ATP-binding site: the N, G1, F, and G2 boxes (4, 7).

Despite the similarities, there are also interesting differences in residue composition between histidine kinases and ATPases that likely delineate their divergent functions. CheA does not contain an analog of an essential glutamate in the GHL ATPases (7), presumed to be the general base involved in water activation for ATP hydrolysis (8). However, the CheA phosphotransfer domain (P1) contains a conserved glutamate adjacent to the phospho-accepting histidine (Glu-67 in *T. maritima* and Glu-70 in *Escherichia coli* and *Salmonella typhimurium*) (9). In *S. typhimurium*, mutation of Glu-70 to Ala abolishes CheA activity (6). Thus, this glutamate may tune the reactivity of the phospho-accepting histidine in a manner similar to the water-activating glutamate of the GHL-ATPases (7).

The properties of the CheA phospho-accepting histidine (residue 48 in *E. coli* or 45 in *T. maritima*) deviate from those of typical solvent-exposed histidines. NMR spectroscopy showed His-48 to have a higher than normal pK_a of 7.8 (9). Furthermore, a hydrogen bond to His-48 $N^{\delta 1}H$ locks the imidazole ring in the $N^{\delta 1}H$ unfavored tautomeric form, even at pH values above its pK_a (9). Crystal structures of the phosphotransfer domain, P1, implicated a glutamate residue (67 and 70 in *T. maritima* and *S. typhimurium*, respectively) as a hydrogen bond acceptor for the phospho-accepting histidine (6, 10). A group of conserved residues (Glu-67, Lys-48, and His-64 in *T. maritima*) also forms a hydrogen bond network with His-45 that could modulate its reactivity (10). Herein, we present biochemical studies of mutants of the *T. maritima* CheA P1 domain that disrupt hydrogen-bonding networks surrounding the phospho-accepting histidine. Biochemistry, crystallography, and NMR spectroscopy were combined to define how local hydrogen bonds activate the CheA histidine for phosphotransfer.

EXPERIMENTAL PROCEDURES

Protein Cloning, Expression, and Purification—T. maritima full-length CheA, Δ289 (domains P3, P4, and P5, residues 290–671), do-

* This work was supported by National Institutes of Health Grants R01-AI 19296 (to M. I. S.), 5R01GM059544-25 (to F. W. D.), and R01-GM066775 (to B. R. C.), an National Institutes of Health predoctoral fellowship (to C. M. Q.), and a Cornell Presidential Research Scholars stipend (to C. G.). The costs of publication of this article were defrayed in part by the payment of page charges. This article must therefore be hereby marked "*advertisement*" in accordance with 18 U.S.C. Section 1734 solely to indicate this fact.

‖ To whom correspondence should be addressed: Division of Biology 147-75, California Institute of Technology, 1200 E. California Blvd., Pasadena, CA 91125. Tel.: 626-395-3944; Fax: 626-796-7066; E-mail: simonm@caltech.edu.

[1] The abbreviations used are: GHL, GyrB, Hsp90, MutL; PEG, polyethylene glycol; AmAc, ammonium acetate; HSQC, heteronuclear single quantum coherence; NOESY, nuclear Overhauser effect spectroscopy.

main P1 and its mutants (residues 4–133), and the truncated P1 variants P1E67Q$_{short}$, P1K48A$_{short}$, and P1H64A$_{short}$ (residues 4–104) were subcloned in the vector pET28(a) (Novagen), transformed, and expressed in *E. coli* strain BL21(DE3) (Novagen). Full-length P1 domain constructs were used in all biochemical assays. P1 short constructs were utilized for crystallization trials. Crystals were obtained only by removing the region corresponding to the fifth helix (residues 105–133) in *S. typhimurium* P1. Protein purification was achieved by affinity chromatography on nickel-nitrilotriacetic acid beads (Qiagen) and gel filtration as described previously (7). Mutations were introduced using the QuikChange site-directed mutagenesis kit (Stratagene).

Phosphorylation Assays—Initial velocities of full-length CheA and its mutants CheA E67Q, CheA K48A, CheA H64A (2–10 μM), or P1 (30 μM) incubated with CheA Δ289 (2 μM) were measured in 50 mM Tris, pH 8.5, 50 mM KCl, and 2 mM dithiothreitol at 50 °C. The initial velocities of full-length CheA and CheA H64A were also compared with one another at room temperature in the same buffer at pH 7.5. Reactions were initiated upon the addition of [γ-^{32}P]ATP. At specific time intervals, aliquots were quenched with 2% SDS electrophoresis buffer containing 25 mM EDTA. Samples were then electrophoresed on 12–18% Criterion Tris-HCl gels (Bio-Rad) using a Criterion Dodeca cell (Bio-Rad). Gels were dried under vacuum and phosphorylation-quantified using a Storm PhosphorImager (Amersham Biosciences). The pH dependence studies were performed in the same manner over a pH range of 6.5–9.6. The same protocol was used when P1 (30 μM) was incubated with Δ289(2 μM) in the presence of a 10-fold excess of P1 mutant (300 μM) or the control bovine serum albumin (300 μM).

Crystallization, Data Collection, Structure Determination, and Refinement—Orthorhombic crystals belonging to the P222$_1$ space group were obtained by mixing 2 μl of 7–15 mg/ml protein with 2 μl of the reservoir solution (14% PEG 2000, 0.1 M NaAc, pH 4.5, 0.2 M AmAc for P1E67Q$_{short}$; 32% PEG 4000, 0.1 M NaAc, pH 4.5, 0.2 M AmAc for P1K48A$_{short}$; 30% PEG 4000, 0.1 M NaAc, pH 4.5, 0.2 M AmAc for P1H64A$_{short}$). Crystals were briefly soaked in a cryoprotectant solution (36% PEG 8000, 0.1 M NaAc, pH 4.5, and 0.2 M AmAc) and then flash-frozen with liquid nitrogen. Diffraction data were collected at the Cornell High Energy Synchrotron Source (CHESS) on beamline A1 (λ = 0.9363 Å) to 1.1, 1.4, and 1.25 Å resolution for P1E67Q$_{short}$, P1H64A$_{short}$, and P1K48A$_{short}$, respectively. Data were processed, scaled, and reduced using the DENZO/SCALEPACK suite of programs (11) (see Table I).

Crystals were isomorphous with those of the wild-type *T. maritima* P1 domain (10), and as such, this model (Protein Data Bank code: 1TQG) served as a starting point for refinement. Based on model phases, the "warpNtrace" feature of ARP/wARP v 5.0 (12) was used to automatically build the initial protein model of E67Q (one molecule per asymmetric unit in all cases). For E67Q and the other mutants, iterative cycles of refinement using the program SHELXL (13) and manual rebuilding of the model in XtalView (14) were used to generate protein models (see Table I). As previously observed in the wild-type structure of P1 (10), several discrete residues (14, 16, 39, 51, 54, and 55) exist in alternate conformations. Extended regions of helices A and D (residues 21–32 and 82–105) also display alternate conformations. Atomic resolution refinement of the E67Q structure (1.1 Å resolution) including the addition of riding hydrogen atoms and anisotropic individual thermal factors was carried out with SHELX (13), as described for the wild-type P1 structure (10).

NMR Spectroscopy—NMR experiments were performed on a 600-MHz Inova spectrometer equipped with ^{1}H [^{13}C/^{15}N] pulsed-field gradient probes. NMR samples contained 50 mM sodium phosphate, 0.05% sodium azide, and 10% D_2O. All experiments were recorded at 50 °C. Assignments for all non-proline backbone amides of wild-type P1 were obtained from D. J. Hamel and F. W. Dahlquist. For this work, three-dimensional ^{15}N-NOESY-HSQC and two-dimensional ^{1}H-^{15}N HSQC correlation experiments were acquired on uniformly ^{15}N-labeled proteins (15). For amide (imidazole) HSQC spectra, the ^{15}N carrier frequency was set to ~121 (190) ppm, using a delay of 4.8 (50) ms to refocus chemical shift evolution arising from the coupling between the backbone amide proton and nitrogen (carbon-bound proton and imidazole nitrogen). In all correlation experiments, 100 (128) complex t_1 increments were recorded. Spectral widths were 1600 (4800) Hz in F_1 and 8000 Hz in F_2. The number of scans in individual two-dimensional experiments ranged from 4 to 128 depending on the signal-to-noise ratio. Quadrature detection in the ^{15}N dimension used the States-TPPI (time-proportional phase incrementation) method (16). Three-dimensional ^{15}N-NOESY-HSQC spectra were recorded for each mutant and used to verify backbone amide resonance assignments. These spectra had the same parameters listed above with 64 complex t_2 increments, spectral width of 8000 Hz in F_3, and a 150-ms mixing time. In the pH titration experiments, a series of spectra were recorded for each protein, ranging from approximately pH 4 to 10. The pH was adjusted with small amounts of HCl or NaOH. HSQC experiments centered at 121 ppm in nitrogen were used to measure chemical shift changes with pH of the amides. HSQC experiments centered at 190 ppm were used to measure pH-dependent chemical shift changes of the histidine rings. All data were processed using the FELIX software package from MSI. The pK_a values of the imidazole rings and the fraction of each histidine tautomer were calculated as described previously (9).

RESULTS AND DISCUSSION

The Hydrogen-bonding Network Surrounding His-45 Optimizes Phosphotransfer—Mutations of Glu-67 to Gln, Asp, and Ala were used to probe whether the hydrogen-bonding ability or negative charge of Glu were critical for phosphorylation of P1 by the kinase domain. The phosphorylation level of wild-type protein was compared with that of mutant protein following a 30-min incubation with [γ-^{32}P]ATP *in vitro*. Mutations were made both in full-length CheA and in the isolated phosphotransfer domain, P1. CheA containing the mutations E67Q, E67D, and E67A showed dramatically reduced autophosphorylation activity (5.7, 8.4, and 2.4%, respectively). The same mutants in separate P1 domains produced even larger reductions in phosphotransfer activity (~ 1% of wild type) when assayed with a protein containing CheA domains P3, P4, and P5 (CheAΔ289).

Although the E67A mutation in *S. typhimurium* has been shown to reduce the ATP phosphotransfer rate (6), these experiments did not distinguish whether the decrease in activity was due to the disruption of secondary structure, the loss of binding between the P1 and the kinase domain, or a catalytic defect. In 10-fold excess, P1E67Q reduces phosphate transfer from wild-type Δ289 to wild-type P1 by more than 70%. The addition of control proteins, such as bovine serum albumin, reduced activity by less than 10%. Assuming a competitive mechanism and taking a measured K_m value for wild-type P1 of 100–250 μM (10), this level of inhibition under presaturation conditions indicates that E67Q interacts with a K_m value within a factor of 2 when compared with wild type. This minimal defect in K_m value cannot account for the low phosphotransfer activities of the conservative mutations E67Q and E67D. Thus, these results suggested that there are stringent requirements on the length, charge, and hydrogen-bond accepting capability of residue 67.

The phosphorylation of P1 by Δ289 has a pH dependence that suggested the phospho-accepting histidine has an elevated pK_a when compared with that of an average solvent-exposed histidine (data not shown). Indeed, the pH dependence of P1 phosphorylation at 50 °C correlates with the fraction of deprotonated histidine present only if the histidine pK_a is increased to 6.9 from 5.9, the estimated pK_a value of a solvent-exposed histidine at 50 °C (9). At pH 6.5, wild-type P1 became phosphorylated to only ~20% of the maximum level observed at pH 8.5. In contrast, the phosphotransfer reactions of the three Glu-67 mutants reflected a more typical pK_a for His-45 in that they are pH-independent above pH 6.0 (data not shown).

The conserved hydrogen-bonding network involving His-45 was disrupted by the mutations K48A and H64A. The activity of CheA H64A was ~15-fold greater than K48A and roughly 270-fold greater than E67Q at 50 °C, pH 8.5. The activity of wild-type CheA was too rapid to be measured under these conditions. At pH 7.5 and room temperature, the initial velocity of wild-type CheA was ~60-fold greater than CheA H64A. A 10-fold excess of K48A reduced the phosphotransfer to wild-type P1 by 44%, indicating that this mutant still competes for the CheA kinase domain but with weaker affinity when compared with wild type or E67Q.

Diminished phosphorylated P1 (P1-P) in our assays could reflect a reduction in phosphorylation by the kinase or a de-

crease in P1-P stability. However, mutations at Lys-48, His-64, or Glu-67 do not affect phosphoramidate bond stability (data not shown), and neither P1K48A nor P1E67Q affects the phosphotransfer activity to the response regulator CheY (6). Thus, there appeared to be no direct effect of the Lys-His-Glu triad on phospho-histidine stability.

High Resolution Structures of P1 Mutants Reveal a Disrupted Hydrogen-bonding Network—To structurally characterize the mutants P1E67Q, P1K48A, and P1H64A, we have determined the crystal structures of their truncated forms, termed short (residues 4–104) to high resolution (for details, see Table I and "Experimental Procedures"). All mutants retain the overall four-helix bundle fold of wild-type P1 (6, 10, 17) with structural changes limited to side-chain conformations near the active histidine.

TABLE I
Summary of data collection and refinement statistics

	$P1E67Q_{short}$	$P1H64A_{short}$	$P1K48A_{short}$
Data collection statistics			
Resolution (Å)	1.1	1.40	1.25
Wavelength (Å)	0.9161	0.9363	0.9363
Total reflections	295,210	176,130	227,281
Unique reflections	37261	18854	25909
Completeness (%)	98.5 (90.0)[a]	98.1 (87.3)	97.6 (98.3)
I/σ(I)	10.4 (2.0)	20.7 (2.7)	29.0 (4.1)
R_{sym} (%) [b]	0.133 (0.393)	0.09 (0.49)	0.063 (0.288)
Mosaicity	0.519	0.584	0.367
Wilson B (Å^2)	19.2	28.1	26.2
Refinement statistics			
Resolution limits (Å)	30–1.1	20–1.4	30–1.25
R_{work} [c]	0.158	0.173	0.192
R_{free} [d]	0.204	0.260	0.253

[a] Numbers in parentheses correspond to values in the highest resolution shell.
[b] $R_{sym} = (\Sigma_{hkl}\Sigma_i|I_i(hkl) - \langle I(hkl)\rangle|)/(\Sigma_{hkl}\Sigma_i\, I(hkl))$.
[c] $R_{work} = \Sigma(||F_{obs}| - |F_{calc}||)/\Sigma|F_{obs}|$.
[d] R_{free} is the R-factor calculated for a 5% test set of reflections excluded from the refinement calculation.

The crystal structure of $P1E67Q_{short}$ (helices A–D) was determined to atomic (1.1 Å) resolution (Table I). The Gln-67 side-chain amide rotates around $\chi_3 - 30°$ from the position held by the Glu-67 carboxylate in wild-type P1. This movement disrupts the conserved hydrogen-bonding network involving His-45, Glu-67, Lys-48, and His-64 (Fig. 1). The $N^{\delta1}$ atom of the phospho-accepting His-45 still hydrogen-bonds to the Gln-67 carbonyl oxygen (2.82 Å), but the His imidazole ring is not co-planar with the glutamine amide, unlike its alignment with the Glu-67 carboxylate in wild-type P1 (Fig. 1*B*). The altered position of the Gln-67 amide allowed the amide nitrogen to hydrogen-bond with two water molecules (2.83 and 3.15 Å). Note that both His-45 imidazole nitrogens should be protonated at the conditions of crystallization (pH 4.5). Although Gln-67 is within hydrogen-bonding distance to $N^{\delta1}$ of the phospho-accepting histidine under these conditions, the distorted geometry and longer hydrogen bond of this interaction indicated that it has weakened relative to the wild type.

Discontinuous density surrounding the phosphorylation site of the K48A mutant indicated that Lys removal destabilizes the positions of Glu-67 and His-64. In particular, His-64 has two alternate conformations, neither of which hydrogen-bond to Glu-67 (Fig. 1, *D* and *E*). When compared with the native configuration, the two His-64 conformers swiveled about angle

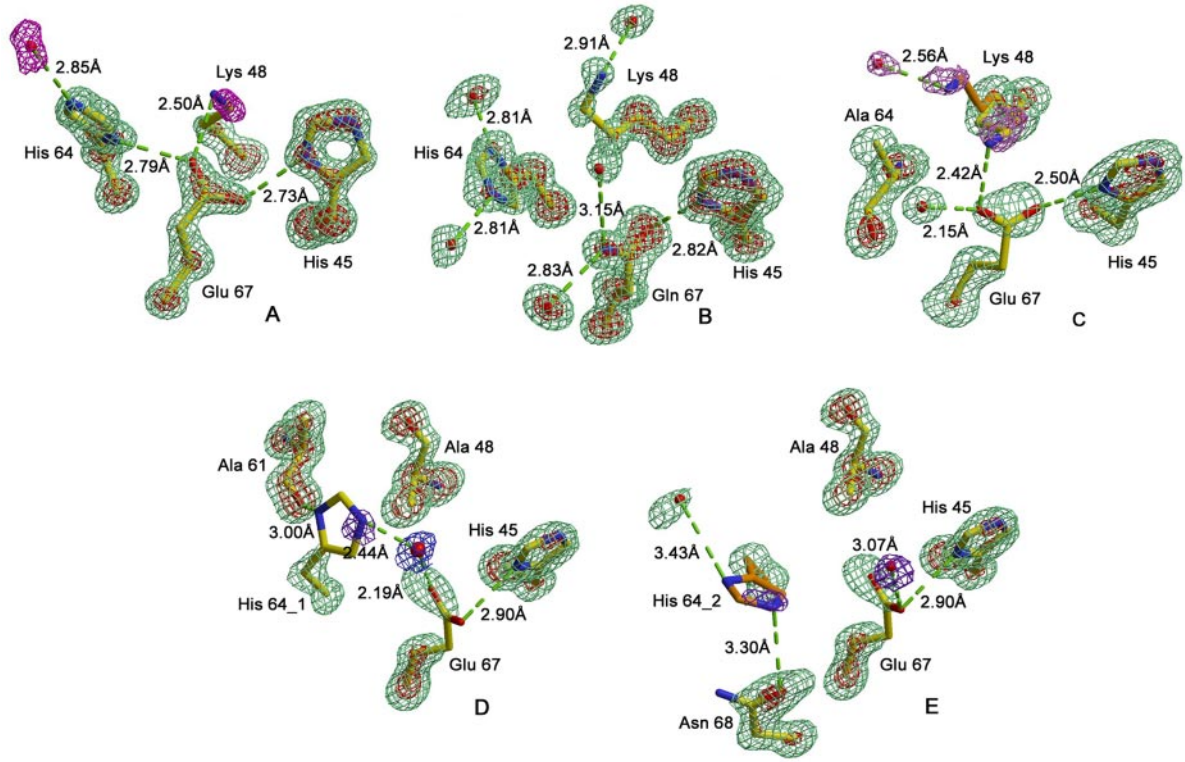

FIG. 1. **The hydrogen-bonding environment surrounding the phospho-accepting histidine of wild-type $P1_{short}$ (*A*), $P1E67Q_{short}$ (*C*) $P1H64A_{short}$ (*B*), and $P1K48A_{short}$ (*D–E*).** *A*, in wild-type P1 (Protein Data Bank code: 1TQG), Glu-67 hydrogen-bonds to both the substrate His-45 and the substrate His-64 in a roughly planar arrangement. *B*, in the E67Q mutation, the hydrogen bond between Glu-67 and His-64 is disrupted, whereas the interaction of Gln-67 to His-45 distorts and lengthens. *C*, in the H64A mutant, the hydrogen bond network is destabilized and, as a result, the side chains show less discernible density. This effect accentuates in the K48A mutant, where His-64 has two alternate conformations (*D* and *E*). However, in all structures, the position of His-45 is relatively unchanged. The $F_o - F_c$ omit electron density maps are contoured between 3–3.5 σ (*red*), 1.4–2.0 σ (*green*), 1.0 σ (*blue*), and 0.71–1.2 σ (*violet*). Each structure is shown from roughly the same perspective by aligning Cα positions of the four active site residues; however, slight adjustments have been made to prevent overlap of the experimental electron density. The figure was produced using Raster3D (28).

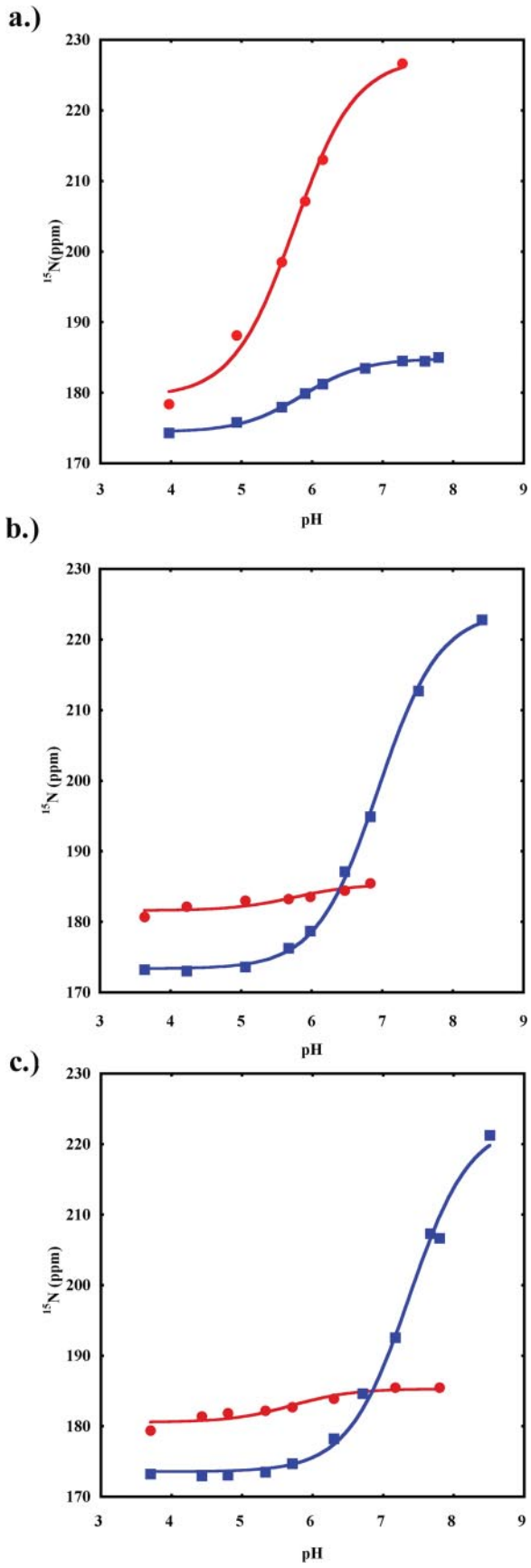

FIG. 2. **The pH titration of the His-45 imidazole ring of the CheA histidine phosphotransfer domain as determined by two-dimensional NMR.** Histidine imidazole groups equilibrate between the completely protonated state and the $N^{\delta 1}H$ and $N^{\epsilon 2}H$ tautomers. The chemical shifts of the His-45 $N^{\delta 1}H$ (●) and $N^{\epsilon 2}H$ (■) atoms of P1E67Q (*a*), P1H64A (*b*), and P1K48A (*c*) as a function of pH show that the E67Q mutation switches the dominant tautomeric state of deprotonated His-45 from $N^{\delta 1}H$ to $N^{\epsilon 2}H$. pK_a values were determined by curve fits to a standard expression for proton ionization, as described previously (9).

TABLE II
The pKa values and predominant tautomeric states of the phosphoaccepting histidine in Thermotoga maritima P1, its variants, and the homologous HPt domain $ArcB_c$

		pK_a [a] (50 °C/30 °C)	Predominant tautomeric state	$N\delta^1H$:$N\epsilon^2H$
P1	His-45	6.9/7.8 [b]	$N^{\delta 1}H$	2.6:1
P1K48A	His-45	6.8/ND [c]	$N^{\delta 1}H$	2.6:1
P1H64A	His-45	6.9/ND [c]	$N^{\delta 1}H$	2.7:1
P1E67Q	His-45	5.8/ND [c]	$N^{\epsilon 2}H$	1:3.3
$ArcB_c$	His-717	NA/6.5 [d]	$N^{\epsilon 2}H$	1:1

[a] Histidines have a temperature dependent heat of ionization. pKa values of free His are 6.5 at 30 °C degrees, but 5.9, at 50 °C (9).
[b] Value measured for *E. coli* P1 at 30 °C (9).
[c] ND, not determined.
[d] NA, not available.

χ_1 by −42 and 121° degrees, one conformer hydrogen bonding to a water molecule (2.4 Å) and the Ala-61 residue (3.0 Å), and the other hydrogen bonding to the neighboring residue Asn-68 (3.3 Å) and another water molecule (3.4 Å). In response, the Glu-67 carboxylate rotated but still hydrogen-bonded to the $N^{\delta 1}$ atom of His-45 (2.9 Å). Although removal of Lys-48 destabilized the conformations of Glu-67 and His-64, the position of His-45 was largely unaffected.

The structural changes incurred by the H64A mutation are not as disruptive as those observed for K48A (Fig. 1*C*). Glu-67 remained hydrogen-bonded to the His-45 $N^{\delta 1}$ (2.5 Å) but had a slightly altered position Lys-48 is also displaced and hydrogen-bonds to a water molecule (2.5 Å) instead of forming a salt bridge with Glu-67. However, the orientation of His-45 remained largely unchanged. Because none of these mutations perturbed the conformation of His-45 nor drastically affected binding of Δ289, reduced phosphorylation activity does not likely derive from structural effects alone.

Glu-67 Stabilizes the Reactive Protonation Tautomer of His-45—To evaluate how mutations of the residues involved in the hydrogen-bonding network affect the chemical properties of the phospho-accepting histidine, we expressed ^{15}N-labeled P1E67Q, P1K48A, and P1H64A for NMR spectroscopy. In solution, histidine imidazole groups have three protonation states: a charged state and two neutral tautomers $N^{\delta 1}H$ and $N^{\epsilon 2}H$, which undergo fast exchange in solution (18, 19). Chemical shift values for histidine nitrogens report on hydrogen-bonding interactions, protonation, and tautomeric states. The P1 mutants contained two or three histidines: 1) His-45, the site of phosphorylation; 2) His-64, a participant in the hydrogen bond network; and 3) a residual N-terminal histidine introduced by the expression vector. Histidine deprotonation at each site was monitored as a function of pH using two-dimensional ^{1}H-^{15}N HSQC experiments (Fig. 2).

The E67Q mutation of *T. maritima* P1 altered the tautomeric state of the phospho-accepting histidine and shifts the effective pK_a of the imidazole. The pH titration of wild-type *E. coli* P1 showed that His-48 (*T. maritima* His-45) $N^{\epsilon 2}$ deprotonates with an elevated pK_a of 7.8 at 30 °C (9) and 6.9 at 50 °C. As expected, in E67Q, the His-45 imidazole pK_a shifts down to a more typical value of 5.8 (Fig. 2*a* and Table II). Surprisingly, the $N^{\delta 1}$ of His-45 deprotonated instead of $N^{\epsilon 2}$. At pH 3.97, the chemical shift values of $N^{\delta 1}$ and $N^{\epsilon 2}$ (178.4 and 174.3 ppm, respectively) approached the expected value for a protonated imidazole nitrogen (176.5 ppm). At the high pH limit, $N^{\delta 1}$ shifts to 226.7 ppm, whereas $N^{\epsilon 2}$ remains relatively constant at 184.5 ppm

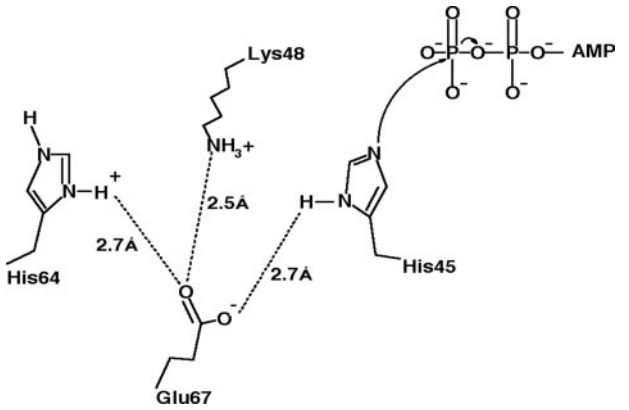

FIG. 3. **Activation of His-45 for phosphoryl transfer.** The hydrogen bond formed between Glu-67 and the $N^{\delta 1}H$ of His-45 stabilizes this otherwise unfavorable histidine tautomer. Glu-67 acts as a general base that activates the active site histidine, making its $N^{\epsilon 2}$ atom more nucleophilic. The P1 domain, therefore, provides a catalytic dyad: an activating glutamate and a phospho-accepting histidine that complete the CheA active site. His-64 and Lys-48 stabilize the position of the catalytic dyad. NMR studies show that His-64 deprotonates at $N^{\delta 1}$ as pH is raised; thus, to maintain hydrogen bonding with Glu-67, the His-64 imidazole ring would have to flip over relative to the conformation observed in the low pH structures.

(Fig. 2*a*). The large change in the $N^{\delta 1}$ chemical shift ($pK_a = 5.8$) indicates that the phospho-accepting histidine primarily exists in the $N^{\epsilon 2}H$ tautomeric state after deprotonation ($N^{\delta 1}H$:$N^{\epsilon 2}H$ tautomeric ratio = 1:3.3; Table II). The difference in charge between Glu and Gln is likely responsible for this effect on histidine reactivity. A negatively charged glutamate carboxylate is a stronger base than a glutamine amide. A Glu in optimal hydrogen-bonding geometry can therefore stabilize an otherwise unfavorable $N^{\delta 1}H$ histidine tautomer over a large pH range.

Similar titration experiments determined that in K48A and H64A, the His-45 imidazole also has properties analogous to native P1 ($pK_a = 6.8$ and, $N^{\delta 1}H$:$N^{\epsilon 2}H = 2.6$:1) (Fig. 2, *b* and *c*; Table II). Thus, of these mutants, E67Q has the most dramatic effect on His-45 reactivity by switching the tautomeric state from $N^{\delta 1}H$ to $N^{\epsilon 2}H$. Presumably, the $N^{\epsilon 2}H$ tautomer cannot position the unprotonated $N^{\delta 1}$ appropriately for nucleophilic attack onto the ATP phosphoryl group bound in the P4 kinase domain.

Chemical and Structural Determinants of Histidine Phosphorylation—CheA phosphorylation requires His-45 to have the $N^{\delta 1}H$ tautomer, and Glu-67 stabilizes this otherwise unfavored protonation state. Although the three mutations studied all affect side-chain positions in the region of the active histidine, these steric changes had minor effects on reactivity when compared with switching the tautomeric state of His-45. For example, K48A is much more active than E67Q, despite this mutation disrupting the conserved hydrogen-bonding network and weakening the K_m for Δ289 to a greater extent. E67Q and H64A both disrupt a hydrogen bond from Lys-48 to either Gln-67 or Glu-67, respectively, but H64A is 270-fold more active than E67Q. Within the catalytic triad of serine proteases, a carboxylate also stabilizes the $N^{\delta 1}H$ tautomer of His (20).

Comparision with GHL-ATPases—In addition to sharing a common fold and ATP-binding site, CheA and GyrB also share common mechanistic features. However, CheA and the GHL family of ATPases differ in the moiety activated by a conserved glutamate residue. In GHL ATPases, a conserved glutamate likely acts as a general base to activate a water molecule for γ-phosphoryl group attack (8). Alternatively, in CheA, a conserved glutamate residue perturbs the phospho-accepting histidine pK_a and stabilizes the normally unfavored $N^{\delta 1}H$ tautomeric state. These effects combine to make His-45 a better nucleophile for phosphate transfer (Fig. 3). The P1 domain provided a catalytic dyad consisting of the nucleophile for phosphate transfer (His-45) and the activating glutamate (Glu-67). Thus, P1 and P4 produces a catalytic center analogous to that of GyrB. Histidine-dependent peptide catalysts have been developed for the specific phosphorylation of small molecules (21, 22). Strategies employed by bacterial histidine kinases to optimize phosphotransfer may be applicable to tuning similar reactivities in such non-biological systems.

Phosphotransfer Mechanisms in Bacterial Signaling—All known histidine phosphotransferase domains display the reactive His on a four-helix bundle scaffold (6, 17, 23, 24). Within these common structural motifs, differences in amino acid composition, electrostatics, hydrogen-bonding networks, and surface properties tunes the reactivity of histidine phosphorylation sites to optimize reactions with phosphotransferase partners. For example, the chemical determinants for histidine phosphorylation differs among monomeric HPt domains from CheA, ArcB ($ArcB_c$), and Ypd1. In contrast to CheA, Ypd1 and $ArcB_c$ accepted a phosphoryl group from the aspartyl phosphate of response regulators instead of from ATP. In these proteins, a Gln hydrogen-bonds to the $N^{\delta 1}H$ atom of the phospho-accepting histidine, which in $ArcB_c$ has the $N^{\epsilon 2}H$ tautomeric state and an unaltered pK_a value (25) (Table II). An equal population of each His protonation tautomer allows for phosphorylation at $N^{\epsilon 2}$ (25). Furthermore, both $ArcB_c$ and Ypd1 mutations of the hydrogen-bonding Gln do not affect histidine phosphorylation (26, 27). Thus, the requirement of a hydrogen-bonded carboxylate for histidine phosphorylation depends on context. In CheA, a carboxylate at position 67 is necessary to stabilize the His-45 $N^{\delta 1}$ tautomer in the chemical environment provided to the reactive His by the entire kinase.

Acknowledgments—We thank the Cornell High Energy Synchrotron (CHESS) for access to data collection facilities.

REFERENCES

1. Parkinson, J. S., and Kofoid, E. C. (1992) *Annu. Rev. Genet.* **26,** 71–112
2. Stock, A. M., Robinson, V. L., and Goudreau, P. N. (2000) *Annu. Rev. Biochem.* **69,** 183–215
3. Inouye, M., and Dutta, R. (eds) (2003) *Histidine Kinases in Signal Transduction*, Academic Press, San Diego, CA
4. Bilwes, A. M., Quezada, C. M., Croal, L. R., Crane, B. R., and Simon, M. I. (2001) *Nat. Struct. Biol.* **8,** 353–360
5. Hirschman, A., Boukhvalova, M., VanBruggen, R., Wolfe, A. J., and Stewart, R. C. (2001) *Biochemistry* **40,** 13876–13887
6. Mourey, L., Re, S. D., Pedelacq, J.-D., Tolstykh, T., Faurie, C., Guillet, V., Stock, J. B., and Samama, J.-P. (2001) *J. Biol. Chem.* **276,** 31074–31082
7. Bilwes, A., Alex, L., Crane, B., and Simon, M. (1999) *Cell* **96,** 131–141
8. Jackson, A. P., and Maxwell, A. (1993) *Proc. Natl. Acad. Sci. U. S. A.* **90,** 11232–11236
9. Zhou, H., and Dahlquist, F. W. (1997) *Biochemistry* **36,** 699–710
10. Quezada, C. M., Gradinaru, C., Simon, M. I., Bilwes, A. M., and Crane, B. R. (2004) *J. Mol. Biol.* **341,** 1283–1294
11. Otwinowski, A., and Minor, W. (1997) *Methods Enzymol.* **276,** 307–325
12. Perrakis, A., Morris, R., and Lamzin, V. S. (1999) *Nat. Struct. Biol.* **6,** 458–463
13. Sheldrick, G. M., and Schneider, T. R. (1997) *Methods Enzymol.* **277,** 319–343
14. McRee, D. E. (1992) *J. Mol. Graph.* **10,** 44–47
15. Zhang, O. W., Kay, L. E., Olivier, J. P., and Formankay, J. D. (1994) *J. Biomol. NMR* **4,** 845–858
16. Marion, D., Ikura, M., Tschudin, R., and Bax, A. (1989) *J. Magn. Reson.* **85,** 393–399
17. McEvoy, M. M., Zhou, H., Roth, A. F., Lowry, D. F., Morrison, T. B., Kay, L. E., and Dahlquist, F. W. (1995) *Biochemistry* **34,** 13871–13880
18. Bachovchin, W. W. (1986) *Biochemistry* **25,** 7751–7759
19. Schuster, I. I., and Roberts, J. D. (1979) *J. Org. Chem.* **44,** 3864–3867
20. Hedstrom, L. (2002) *Chem. Rev.* **102,** 4501–4524
21. Sculimbrene, B. R., Morgan, A. J., and Miller, S. J. (2002) *J. Am. Chem. Soc.* **124,** 11653–11656
22. Sculimbrene, B. R., and Miller, S. J. (2001) *J. Am. Chem. Soc.* **123,** 10125–10126
23. Xu, Q., and West, A. H. (1999) *J. Mol. Biol.* **292,** 1039–1050
24. Kato, M., Mizuno, T., Shimizu, T., and Hakoshima, T. (1997) *Cell* **88,** 717–723
25. Ikegami, T., Okada, T., Ohki, I., Hirayama, J., Mizuno, T., and Shirakawa, M. (2001) *Biochemistry* **40,** 375–386
26. Matsushika, A., and Mizuno, T. (1998) *BioSci. Biotech. Biochem.* **62,** 2236–2238
27. Janiak-Spens, F., and West, A. H. (2000) *Mol. Microbiol.* **37,** 136–144
28. Merritt, E. A., and Murphy, M. E. (1994) *Acta Crystallogr. Sect. D Biol. Crystallogr.* **50,** 869–873